IOP Conf. Series: Earth and Environmental Science **170** (2018) 032127 doi:10.1088/1755-1315/170/3/032127

Numerical study of the storm surges caused by increasing wind speeds in the Bohai Sea, Yellow Sea and East China Sea

Junli Xu[1], Qiang Liu[2, *] and Xianqing Lv[3]

[1]School of Mathematics and Physics, Qingdao University of Science and Technology, Qingdao 266100, China
[2]College of Engineering, Ocean University of China, Qingdao 266100, China
[3]Key Laboratory of Physical Oceanography (Ocean University of China), Ministry of Education, Ocean University of China, Qingdao 266100, China

*Corresponding author e-mail: liuqiang@ouc.edu.cn

Abstract. A coupled tide-surge model, validated for the Typhoon 7203, is used to construct 20 synthetic storm surge cases without and with tides by increasing wind speeds in the Bohai Sea, Yellow Sea and East China Sea. Simulations of Typhoon 7203 and synthetic storm surges are used to study the extreme water elevations at 10 tidal stations along the coast, as well as to evaluate the impacts of increasing wind speeds and tide-surge interactions on storm surge elevations. Results indicate that the increasing wind speeds by 39% can result in at least 103% higher extreme water elevations at 10 tidal stations. Furthermore, the largest differences between storm surge elevations without and with tide-surge interactions can reach 76 and 89 cm at YingKou and LianYunGang tidal station for 60% increase in wind speed, respectively.

1. Introduction

In the Bohai Sea, Yellow Sea and East China Sea, numerous tropical cyclones or typhoons have produced the damaging storm surge, which is an abnormal rise or fall in the seawater level associated with a low pressure weather system. Storm surge and related coastal flooding can result in loss of human life and damage to property [4, 7, 8], and the abnormal low water level mainly destroys maritime safety and coastal engineering.

As some researchers have explored, several factors can influence the height, extent and duration of storm surge, such as tropical cyclone size [2, 5] and pre landfall wind speeds [10]. By increasing the wind speed and changing the landfall location, Sebastian et al.[13] constructed five synthetic storm surge scenarios in the upper Texas coast according to the SWAN + ADCIRC model. Results showed that increasing wind speeds resulted in higher surge and shifting the storm westward caused higher levels of surge due to more intense, higher shore-normal winds. Typhoon-induced storm surge and coastal flooding can be further aggravated by astronomical tides [11, 17]. Using the two-way nested coupled tide-surge model, Zhang et al. [18] explored the impacts of astronomical tides on storm surges in the Taiwan Strait, indicating that the influence should be considered in prediction model. Based on a regional hydrodynamic model, Quinn et al. [12] explored the influence of tide-surge interaction on the surge in the Solent and surrounding waters, and simulation results indicated that their interactions affected the magnitude and timing of the surge.

Nevertheless, in the Bohai Sea, Yellow Sea and East China Sea which are vulnerable to storm surges, the effect of increasing wind speeds on the storm surges has not received much attention. In this study, using a two-dimensional coupled tide-surge model, we will investigate the storm surges without and with tide-surge interactions by increasing wind speeds and explore the influences of tide-surge interactions on storm surge elevations during the Typhoon 7203.

2. Numerical Model

The coupled tide-surge model is developed on the basis of a depth averaged flow model, and the model framework is as below.

In the spherical coordinates, the governing equations used in the present coupled model are composed of the depth averaged equations of continuity and momentum.

$$\frac{\partial \zeta}{\partial t}+\frac{1}{a}\frac{\partial\left[(h+\zeta)u\right]}{\partial \lambda}+\frac{1}{a}\frac{\partial\left[(h+\zeta)v\cos\phi\right]}{\partial \phi}=0, \tag{1}$$

$$\frac{\partial u}{\partial t}+\frac{u}{a}\frac{\partial u}{\partial \lambda}+\frac{v}{R}\frac{\partial u}{\partial \phi}-\frac{uv\tan\phi}{R}-fv+\frac{ku\sqrt{u^2+v^2}}{h+\zeta}-A\Delta u$$

$$+\frac{g}{a}\frac{\partial\left(\zeta-\bar{\zeta}\right)}{\partial \lambda}+\frac{1}{\rho_w a}\frac{\partial P_a}{\partial \lambda}-\frac{\rho_a}{\rho_w}\frac{C_d W_x\sqrt{W_x^2+W_y^2}}{h+\zeta}=0, \tag{2}$$

$$\frac{\partial v}{\partial t}+\frac{u}{a}\frac{\partial v}{\partial \lambda}+\frac{v}{R}\frac{\partial v}{\partial \phi}+\frac{u^2\tan\phi}{R}+fu+\frac{kv\sqrt{u^2+v^2}}{h+\zeta}-A\Delta v$$

$$+\frac{g}{R}\frac{\partial\left(\zeta-\bar{\zeta}\right)}{\partial \phi}+\frac{1}{\rho_w R}\frac{\partial P_a}{\partial \phi}-\frac{\rho_a}{\rho_w}\frac{C_d W_y\sqrt{W_x^2+W_y^2}}{h+\zeta}=0, \tag{3}$$

Where t is time; λ and ϕ are east longitude and north latitude, respectively; u, v are east and north components of the current; h is depth of undisturbed water; ζ is sea surface elevation above the undisturbed level; $h+\zeta$ is total water depth; $\bar{\zeta}$ is the adjusted height of equilibrium tides; R is earth radius and $a=R\cos\phi$; $f=2\Omega\sin\phi$ is Coriolis parameter (here, Ω is angular speed of Earth's rotation); k is bottom friction factor; A is horizontal eddy viscosity coefficient; Δ is Laplace operator and $\Delta(u,v)=a^{-1}\left[a^{-1}\partial_\lambda\left(\partial_\lambda(u,v)\right)+R^{-1}\partial_\phi\left(\cos\phi\partial_\phi(u,v)\right)\right]$; $\rho_w=1025\,\mathrm{kg/m^3}$ is seawater density and $\rho_a=1.27\,\mathrm{kg/m^3}$ is air density; g is gravitational acceleration. The wind-stress coefficient C_d used in this paper is determined from the equation (Wu, 1982):

$$C_d=\begin{cases}\left(0.8+0.065\times U_{10}\right)\times 10^{-3}, & 0<U_{10}<50\mathrm{m/s}\\ 0.0026, & U_{10}>50\mathrm{m/s}\end{cases}. \tag{4}$$

Where U_{10} is the wind velocity measured at 10-m above the mean sea surface. The surface wind field (W_x, W_y) and pressure field P_a are the meteorological driving forces which generate storm surges [1, 18]. Generally, the effect of background wind field on the storm surge elevation is weaker than that of pure tropical cyclone, yet should not be ignored [14, 15]. In the present model, synthetic wind field is obtained by the National Centers for Environmental Prediction (NCEP) reanalysis surface winds data and a storm model [6]. The pressure field for the tropical cyclone is also from Jelesnianski [6].

In this coupled model, initial values of the surface elevation and current velocity are computed by tidal model. It is supposed that no water is permitted to flow into the coast along the closed boundaries. The open boundary conditions are sea-surface elevations, which are as follows:

$$\zeta = \sum_{j=1}^{J} f_j H_j \cos\left(\omega_j t + u_j + v_j - g_j\right), \tag{5}$$

Where H_j and g_j are separately amplitude and phase-lag of the *j*th tidal constituent; ω_j is angular speed; v_j is initial phase angle; f_j is nodal factor; and u_j is nodal angle.

After removing pressure term and wind stress term from equations (2) and (3), the coupled model is simplified to the tidal model of Lu and Zhang [9]. The tidal model is actuated by open boundary conditions and tidal potential. Sea surface level on the open boundary is calculated by equation (5) and tidal potential is computed as Fang et al. [3]. The model starts on April 27, 1972 and runs for 90 days, where the harmonic analysis calculation can be done for the simulated results in the last 60 days. The absolute mean differences of amplitude and phase-lag of sea surface elevation are separately less than 4 cm and 5° between simulated results and observations at the 489 points of TOPEX/Poseidon (T/P) tracks for four principal constituents M2, S2, K1 and O1 [16].

3. Numerical Procedure

3.1. *Model Configuration*

The study area in this paper covers the Bohai Sea, Yellow Sea and East China Sea, and the first island chains and Taiwan Strait are as open boundaries. The tides in the coupled model include eight principal constituents (M2, S2, K1, O1, N2, K2, P1, Q1). The computational domain runs from 117.5°E to 131.5°E and 24°N to 41°N in the numerical simulations, and bathymetry data is from E-TOP-5. The spherical grid is 5′×5′. The time step is taken as 60 s.

The present model can be used to calculate three water elevations: storm surge without the impact of tide (denoted by storm surge model); the tide only (denoted by tidal model); and total water elevation which considers both the tide and meteorological forcing (denoted by coupled tide-surge model) [18]. To obtain the storm surges with tide-surge interactions, the model will be run twice: once to calculate the tide only, and once to compute the total water elevation. Subtracting the tide from the total water elevation, we can obtain the storm surge elevation time series with the coupling effect of tide-surge. Besides, the storm surge elevation without tide-surge interactions is simulated by the storm surge model

3.2. *Case Description*

In this paper, we investigate the impacts of increasing wind speeds on the storm surges without and with tides during the Typhoon 7203 in the Bohai Sea, Yellow Sea and East China Sea. The trajectory of Typhoon 7203 (from July 25th to 28th, 1972) and locations of 10 tidal stations are shown in Fig.1. The typhoon data is available every 6 hour in here.

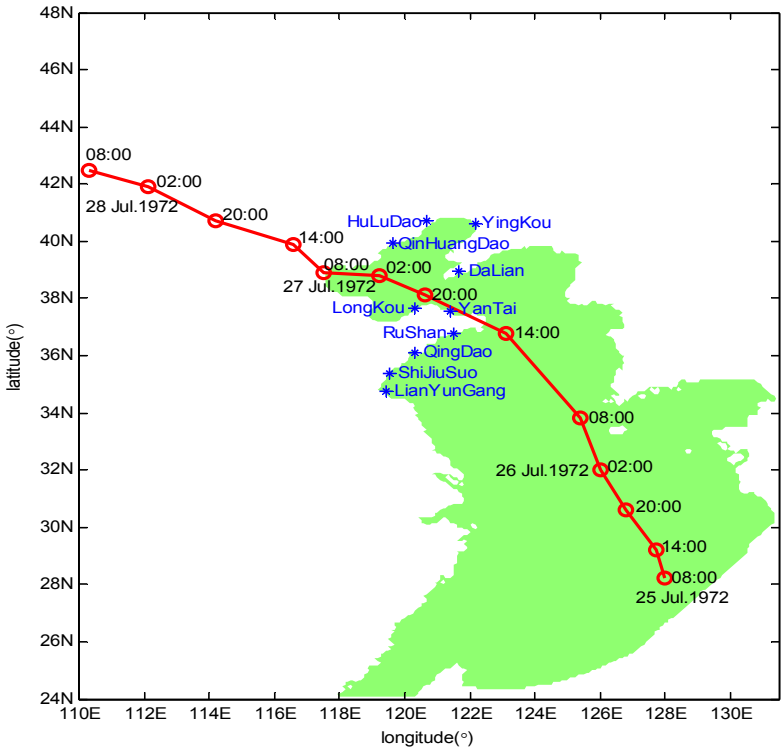

Figure 1. The blue asterisks denote the locations of tidal stations, red solid lines are the trajectory of Typhoon 7203, and red circles indicate time series of the typhoon.

In order to evaluate the effect of increasing the wind speed on the storm surge, 20 synthetic storm surge cases without and with tides are constructed when all the other conditions are the same. In other words, there are 21 different storm surge cases when including the actual wind field. The specific processes are determined by the following steps. In the first case (hereafter, Case 1), it is assumed that the wind speed used in the model is the actual wind speed, symbolized by W_1. From the second case (hereafter, Case 2) to the last one (hereafter, Case 21), the synthetic wind speed W_i can be represented by the following equation:

$$W_{i+1} = (1 + i \times 3\%) \times W_1, \quad i = 1,...,20 .$$

4. Results and Discussion

In this section, the results of the numerical simulation will be exhibited in several ways. Each illustrates a different aspect of the effects of increasing wind speeds on the storm surge elevations without and with tides, and the influences of tide-surge interactions on the storm surge elevations under different wind speed conditions.

4.1. *Extreme Water Elevations of 21 Cases*

Storm surge elevations without tides of 21 cases can be calculated by running the storm surge model in the Bohai Sea, Yellow Sea and East China Sea during the Typhoon 7203. Fig.2 (left) shows the extreme values of 21 storm surge elevations at 10 tidal stations. When considering the tides, the extreme values of 21 storm surge elevations with the tide-surge interactions is also shown in Fig.2 (right).

As you can see from Fig.2, the effects of increasing wind speeds on the storm surge elevations without and with tide-surge interactions are very obvious. The increasing wind speeds by 39% can

result in at least 103% higher extreme water elevations at 10 tidal stations. But only a 36% increase in wind speed yields at least 103% a higher extreme value after considering the tide-surge interactions. The results indicate that the impact of tide-surge interactions on extreme water elevation of storm surge is remarkable as the wind speed increases.

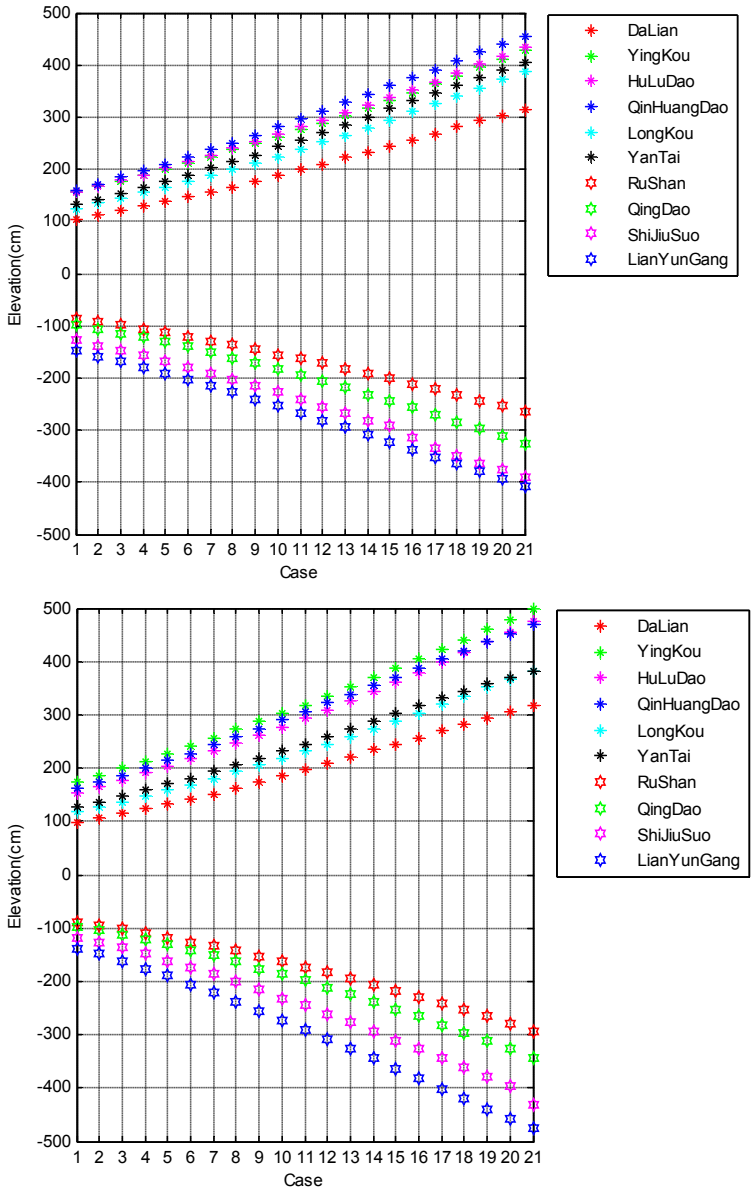

Figure 2. Extreme values (cm) of 21 storm surge elevations without (left) and with (right) tide-surge interactions at 10 tidal stations.

4.2. *Time Series of Storm Surge Elevations*

Through comparing the results in Fig.2 (left and right), differences between extreme values of 21 storm surge elevations without and with tide-surge interactions are larger at Ying Kou tidal stations for the rising water, and at LianYun Gang tidal station for the falling water. Therefore, simulation results in these two tidal stations will be analyzed.

For the numerical simulations in Case 1, Case 6, Case 11, Case 16 and Case 21, storm surge elevations without and with tide-surge interactions at Ying Kou and LianYun Gang tidal stations are

shown in Fig.3 (left) and Fig.4 (left), respectively. The results indicate that storm surge elevations increase with increasing wind speed in these two tidal stations, but little variation in shape or timing of the hydrograph. Fig.3 (right) and Fig.4 (right) present the differences between the storm surge elevations without and with tide-surge interactions in above-mentioned five cases at Ying Kou and LianYun Gang tidal stations. It can be seen that the effects of tide-surge interactions on storm surge elevations become more obvious as the wind speed increases gradually. When wind speed has a 60% increase, the largest difference is even up to 76 cm and 89 cm in these two tidal stations, respectively.

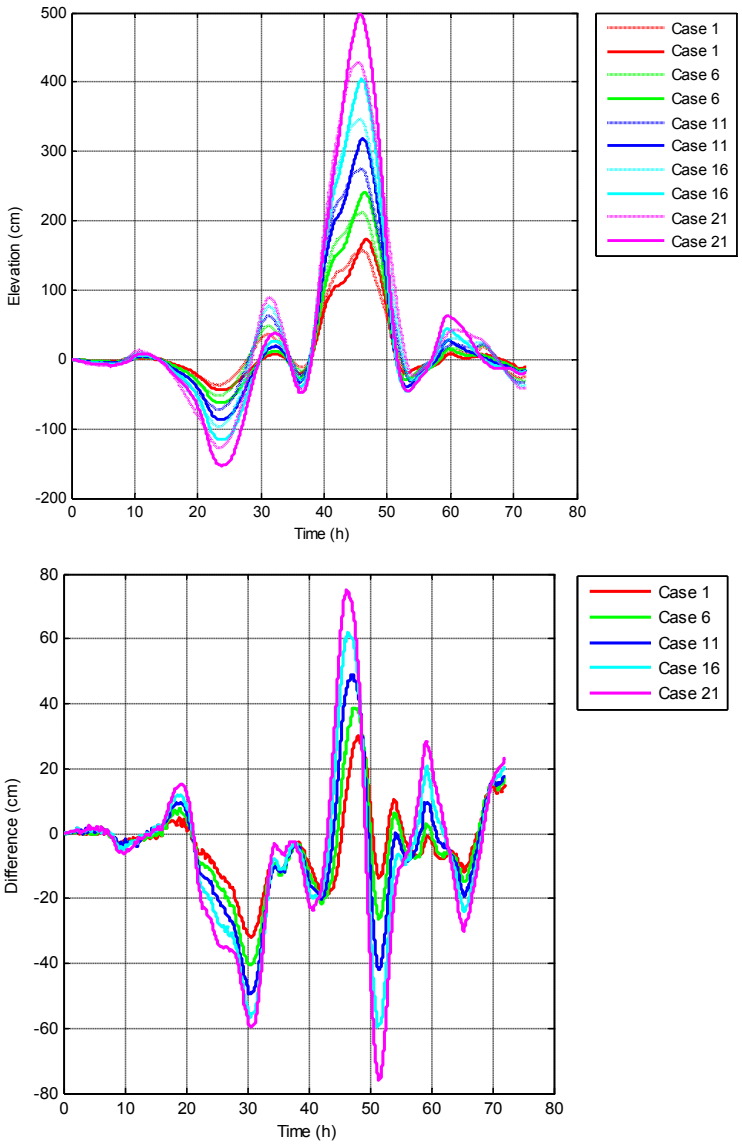

Figure 3. Comparison of storm surge elevations (left) and differences (right) without (dotted lines) and with (solid lines) tide-surge interactions in Case 1 (red line), Case 6 (green line), Case 11 (blue line), Case 16 (cyan line) and Case 21 (mauve line) at YingKou tidal stations.

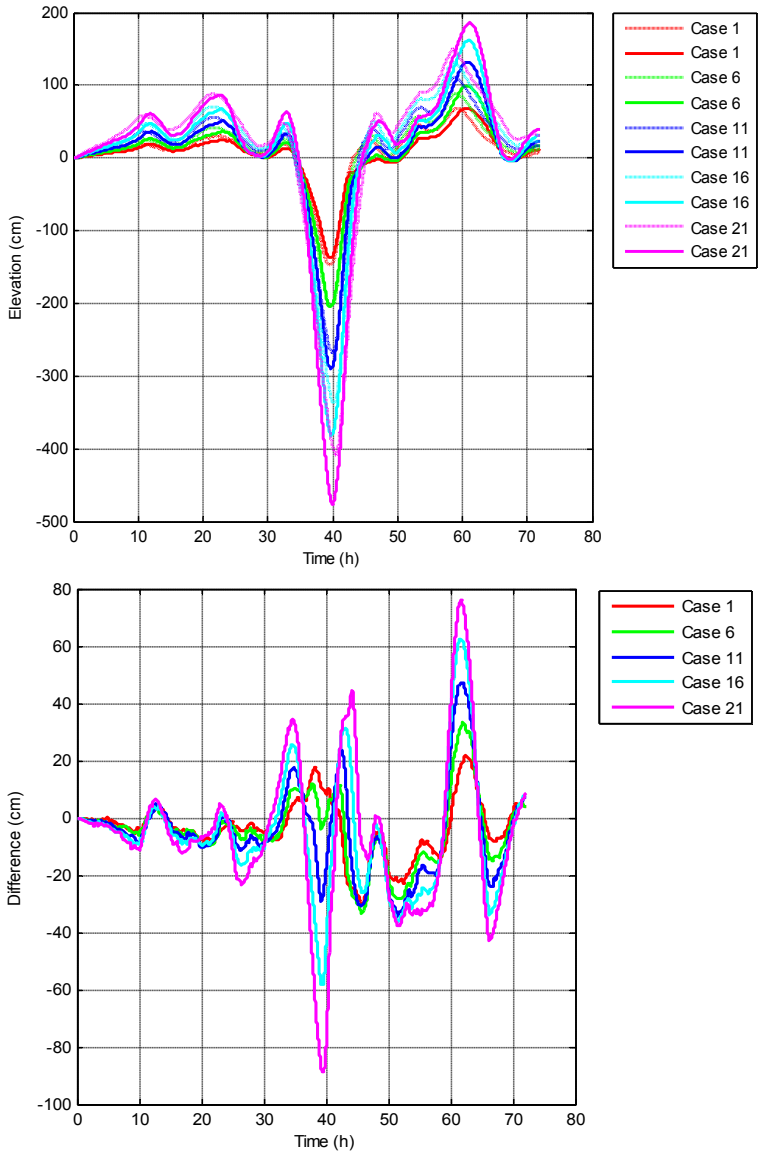

Figure 4. Comparison of storm surge elevations (left) and differences (right) without (dotted lines) and with (solid lines) tide-surge interactions in Case 1 (red line), Case 6 (green line), Case 11 (blue line), Case 16 (cyan line) and Case 21 (mauve line) at LianYunGang tidal stations.

5. Summary and Conclusion

This paper used a coupled tide-surge model to analyze the storm surge in the Bohai Sea, Yellow Sea and East China Sea during the Typhoon 7203. In the coupled model, the tide was introduced by the tidal potential and open boundary conditions, and the wind stress was given by a synthetic wind field. The storm surge elevations without and with tide-surge interactions were simulated under increasing wind speeds in the whole sea areas.

In order to investigate the impacts of increasing wind speeds on storm surge elevations, storm surge elevations of 21 cases without and with tide-surge interactions were calculated in the whole sea areas. Meanwhile, the extreme water elevations at 10 tidal stations along the coast were analyzed. The results showed that increasing wind speed by 39% caused extreme water elevations of storm surges without tide-surge interactions to increase by at least 103%, but only 36% increase in wind speed for storm surge with tide-surge interactions. Furthermore, storm surge elevations without and with tide-surge

interactions in YingKou and LianYun Gang tidal stations were analyzed, indicating that storm surge elevations increased with increasing wind speed, but little variation in shape or timing of the hydrograph.

The differences between storm surge elevations without and with tide-surge interactions were also calculated with the purpose of estimating the tide-surge interactions. For example, at YingKou and LianYunGang tidal station, the largest differences were 76 and 89 cm as the wind speed increased by 60%, respectively, demonstrating that the tide-surge interactions must be considered.

Acknowledgements
Partial support for this research was provided by the National Natural Science Foundation of China through grant 41606006, Opening Fund of Shandong Provincial Key Laboratory of Marine Ecology and Environment & Disaster Prevention and Mitigation through grant 201411, the national key research and development plan through grant 2016YFC1402304 and the key research and development plan of Shandong Province through grant 2016ZDJS09A02.

References

[1] Chen W B, Liu W C, Hsu M H. 2012. Predicting typhoon-induced storm surge tide with a Two-dimensional hydrodynamic model and artificial neural network model. *Natural Hazards and Earth System Sciences*, **12**: 3799-3809.
[2] Dietrich J C, Coauthors. 2011. Modeling hurricane waves and storm surge using integrally-coupled, scalable computations. *Coastal Engineering*, **58**: 45-65.
[3] Fang G H, Kwok Y K, Yu K J, Zhu Y H. 1999. Numerical simulation of principal tidal constituents in the South China Sea, Gulf of Tonkin and Gulf of Thailand. *Continental Shelf Research*, **19**: 845-869.
[4] Haigh I D, Wijeratne E M S, MacPherson L R, Pattiaratchi C B, Mason M S, Crompton R P, George S. 2014. Estimating present day extreme water level exceedance probabilities around the coastline of Australia: tides, extra-tropical storm surges and mean sea level. *Climate Dynamics*, **42**: 121-138.
[5] Irish J L, Resio D T, Ratcliff J J. 2008. The influence of storm size on hurricane surge. *Journal of Physical Oceanography*, **38**: 2003-2013.
[6] Jelesnianski C P. 1965. A numerical calculation of storm tides induced by a tropical storm impinging on a continental shelf. *Monthly Weather Review*, **93** (6): 343-358.
[7] Lin N, Emanuel K, Oppenheimer M, Vanmarcke E. 2012. Physically based assessment of hurricane surge threat under climate change. *Nature Climate Change*, **2**: 462-467.
[8] Liu H Q, Zhang K Q, Li Y P, Xie L A. 2013. Numerical study of the sensitivity of mangroves in reducing storm surge and flooding to hurricane characteristics in southern Florida. *Continental Shelf Research*, **64**: 51-65.
[9] Lu X Q, Zhang J C. 2006. Numerical study on spatially varying bottom friction coefficient of a 2D tidal model with adjoint method. *Continental Shelf Research*, **26**: 1905-1923.
[10] Needham H F, Keim B D. 2014. An empirical analysis on the relationship between tropical cyclone size and storm surge heights along the U.S. Gulf Coast. *Earth Interactions*, **18** (8): 1-15.
[11] Olbert A I, Nash S, Cunnane C, Hartnett M. 2013. Tide-surge interactions and their effects on total sea levels in Irish coastal waters. *Ocean Dynamics*, **63**: 599-614.
[12] Quinn N, Atkinson P M, Wells N C. 2012. Modelling of tide and surge elevations in the Solent and surrounding waters: The importance of tide-surge interactions. *Estuarine, Coastal and Shelf Science*, **112**: 162-172.
[13] Sebastian A, Proft J, Dietrich J C, Du W, Bedient P B, Dawson C N. 2014. Characterizing hurricane storm surge behavior in Galveston Bay using the SWAN + ADCIRC model. *Coastal Engineering*, **88**: 171-181.
[14] Tang J, Shi J, Li X Q, Deng B, Jin M M. 2013. Numerical simulation of typhoon waves with

typhoon wind model. *Transactions of Oceanology and Limnology*, **2**: 24-30 (in Chinese).
[15] Wen B, Wang P, Wan L, Zhang F R. 2008. Experiments on the simulation of typhoon waves in the inshore area of China Sea. *Marine Science Bulletin*, **27** (3): 1-6 (in Chinese).
[16] Xu J L, Zhang Y H, Cao A Z, Liu Q, Lv X Q. 2016. Effects of tide-surge interactions on storm surges along the coast of the Bohai Sea, Yellow Sea, and East China Sea. *Science China Earth Sciences*, **59** (6): 1308-1316.
[17] Yang Z Q, Wang T P, Leung R, Hibbard K, Janetos T, Kraucunas I, Rice J, Preston B, Wilbanks T. 2014. A modeling study of coastal inundation induced by storm surge, sea-level rise, and subsidence in the Gulf of Mexico. *Natural Hazards*, **71**: 1771-1794.
[18] Zhang W Z, Hong H S, Shang S P, Chen D W, Chai F. 2007. A two-way nested coupled tide-surge model for the Taiwan Strait. *Continental Shelf Research*, **27**: 1548-1567.